Pak. J. Bot., 58(7) July, 2026.

ARTICLE DOI: http://dx.doi.org/10.30848/PJB2026-7(11)

GENETIC DIVERSITY, PHYTOCHEMICAL PROFILING, AND ANTIMICROBIAL ACTIVITIES OF *MESEMBRYANTHEMUM FORSKALII* FROM TWO REGIONS OF SAUDI ARABIA

AMINAH Z ALANAZI, ABD EL-ZAHER M.A. MUSTAFA, MOHAMED TARROUM, SALIM KHAN*, ABDEL-RHMAN Z. GAAFAR, ABDULRAHMAN AL-HASHIMI, NORAH S. ALFARRAJ, MOHAMMAD NADEEM AND FAHAD AL-QURAINY

Department of Botany and Microbiology, College of Science, King Saud University, P.O. Box 2455, Riyadh 11451, Saudi Arabia

*Corresponding author's email: salimkhan17@yahoo.co.in

Abstract

Mesembryanthemum forskahlii (Aizoaceae) is a medicinally important and ecologically adaptable species whose genetic and phytochemical diversity remains underexplored. In this study, two natural populations from Aljouf and Qassim (Saudi Arabia) were analyzed to assess genetic variation, genome size, phytochemical composition, and antimicrobial activity. Using 16 ISSR primers, 303 loci were scored, with 99.01% polymorphism, indicating high allelic richness; AMOVA revealed that 78% of genetic variation resided within populations, while Gst (0.1369) and Nm (3.15) indicated moderate differentiation and substantial gene flow. UPGMA and PCoA clustering confirmed partial overlap between populations, reflecting ongoing genetic exchange. Genome size estimation showed small but consistent differences (Aljouf: 0.845 pg; Qassim: 1.059 pg), both within the Aizoaceae range. GC–MS profiling revealed regional variation in secondary metabolites, with Aljouf extracts enriched in n-Hexadecanoic acid 9 14.96%) and Qassim extracts dominated by Lupeol (33.33%). Antibacterial assays demonstrated strong inhibition against *Escherichia coli* (70.28%) and *Staphylococcus aureus* (55.66%), with higher activity in Aljouf extracts, while antifungal effects were most pronounced against *Alternaria alternata* (95%), followed by *Aspergillus terreus* (71%) and *Candida tropicalis* (65%). These findings provide the first integrative evidence of high genetic diversity, conserved genome size, population-specific phytochemical variation, and potent antimicrobial activity in *M. forskalii*, highlighting its adaptive capacity, medicinal potential, and conservation value.

Key words: *Mesembryanthemum forskahlii Hochst. ex Boiss*; ISSR markers; Genetic diversity; Genome size; GC–MS; Phytochemicals; Antimicrobial activity

Introduction

Halophyte plants have become a subject of increasing interest due to their high nutritional value, making them promising crops for food security (Sun *et al*., 2025). In Saudi Arabia, these plants are of considerable importance to local communities for both their medicinal and nutritional benefits. Among them, *Mesembryanthemum forskahlii* Hochst. ex Boiss. (syn. *Opophytum forskahlii* Hochst. ex Boiss.), commonly known as Forskal fig-marigold and locally referred to as "Samh," is a robust, drought-tolerant wild plant that thrives in the deserts of the Middle East and North Africa (Awabdeh *et al*., 2022). Belonging to the genus *Mesembryanthemum*, a group of flowering plants also called ice plants, the species is part of the family Aizoaceae, which is widely distributed in South Africa, the Mediterranean region, South Australia, California, and the Atlantic Islands (Arena *et al.*, 2020). In Saudi Arabia, *M. forskalii* is particularly abundant in the northern regions, such as Aljouf, where it is protected under the King Salman Natural Reserve (KSRNR) (Foudah *et al.*, 2022). Its success in arid environments is largely due to its evolutionary adaptations, which allow it to grow in tropical, subtropical, and desert ecosystems (Abd El-Raouf, 2021).

M. forskalii seeds (samh) served as an important traditional food source for Bedouins, often mixed with dates or used to make bread, especially in times when wheat or other cereals were scarce (Al-Otaibi & Al-Motwaa, 2025; Alderaywsh *et al.*, 2019). Nutritional studies confirm the seeds' value, reporting high levels of proteins, carbohydrates, and fats (Abdel-Hamid *et al.*, 2021). Amino acid profiling revealed the presence of seven essential amino acids at levels higher than those found in wheat and barley (Al-Jassir *et al.*, 1995). The seeds also contain important minerals, including calcium, magnesium, potassium, iron, and zinc (Abdel-Hamid *et al.*, 2021). Comparisons with lentils, corn, wheat, and rice further emphasize their nutritional potential (Mohammed *et al.*, 2023). Collectively, these attributes underscore the significance of *M. forskalii* as both a subsistence and nutritionally rich food plant. Beyond nutrition, the plant contains medicinal compounds like beta-sitosterol, which can lower cholesterol levels (Al Faris *et al.*, 2011). Furthermore, seed extracts of *M. forskalii* are reported to treat fungal infections, particularly scalp-related ailments (Bilel *et al.*, 2020). Samh seed consumption has also been linked to reduced triglyceride and glucose levels (AL-Qahiz, 2009). Its phytochemical composition provides a strong antioxidant profile, attributed to beta-sitosterol and

Received: 25-10-2025 | Revised: 23-11-2025 | Accepted: 05-12-2025 | Online: 11-03-2026

3-methoxy-(3-beta,5-alpha) cholesterin-6-one, which play critical roles in scavenging free radicals and reducing oxidative stress (Bilel *et al.*, 2020; Abdel-Farid *et al.*, 2016; Arivarasu, 2023). Additionally, *M. forskalii* seed oil extracts exhibit notable antibacterial activity. Studies report significant inhibitory effects against several pathogenic bacteria, including *Escherichia coli, Klebsiella pneumoniae, Staphylococcus aureus,* and *Pseudomonas aeruginosa,* using the disk diffusion assay (El-Amier *et al.*, 2021). Similarly, antifungal effects have been observed against *Aspergillus flavus, Aspergillus carneus,* and *Penicillium chrysogenum* (Bilel *et al.*, 2020).

Morphologically, *M. forskalii* is characterized by a short, erect stem that branches from the base and produces small, dark brown seeds (Awabdeh *et al.*, 2022). The seeds are campylotropous, appearing distorted externally but containing a coiled embryo internally (Al-Jassir *et al.*, 1995). They are enclosed in hygroscopic capsules that open upon contact with moisture, facilitating seed dispersal. The flowers are hermaphroditic and insect-pollinated (Mallon, 2012). These features highlight the plant's adaptability to arid landscapes and its evolutionary fitness.

In addition to its nutritional and medicinal properties, *Mesembryanthemum forskalii* represents a valuable genetic resource for arid and semi-arid regions. Despite its ecological, ethnobotanical, and medicinal significance, limited scientific knowledge exists regarding its genetic diversity, phytochemical variability, and bioactive potential, particularly in relation to how environmental variation across Saudi Arabia shapes its genetic structure and functional biochemical traits. Plant populations often exhibit region-specific adaptations, which can lead to variation in secondary metabolites and antimicrobial activities (Labarrere *et al*., 2019; Ogwu *et al*., 2025). Assessing the genetic diversity of wild populations is also critical for conservation planning, especially in light of increasing anthropogenic pressures and climate change, which threaten the genetic integrity of desert plants (Salgotra & Chauhan, 2023). Among the molecular approaches available, inter-simple sequence repeat (ISSR) markers are particularly advantageous due to their ability to generate a high level of polymorphism, cost-effectiveness, reproducibility, and the fact that they do not require prior sequence information (Vijayan, 2005; Mint Abdelaziz *et al*., 2020). These features make ISSRs highly suitable for assessing genetic diversity in non-model and underutilized plant species such as *M. forskalii*. This gap limits our understanding of how regional conditions influence its adaptive potential and antimicrobial value, underscoring the need for a unified molecular and phytochemical assessment. Therefore, this study was designed to provide an integrated evaluation of *M. forskalii* populations from two ecologically distinct regions, Qassim and Aljouf. Specifically, the research aimed to (i) assess genetic diversity using ISSR markers, (ii) characterize and compare the phytochemical profiles of plant extracts, and (iii) evaluate their antibacterial and antifungal activities against selected pathogens. By linking genetic variability with biochemical and antimicrobial properties, this study highlights the adaptive and functional diversity of *M. forskalii* and offers insights to support its conservation and potential application as a source of nutraceuticals and natural antimicrobial agents.

Materials and Methods

Sample collection: Fresh young leaves and seeds of *Mesembryanthemum forskahlii Hochst. ex Boiss* were collected from two regions in Saudi Arabia, Aljouf district (29.8874° N, 39.3206° E) and Al-Rummah Valley in the Qassim district (25.658213° N, 42.658188° E) (Fig. 1). Plant materials from both populations collected in April 2024 were used for DNA extraction, genome size estimation, and phytochemical analysis. Sampling was carried out at about 10 locations per region, with 3–5 individuals sampled from each site. In total, 69 plant samples were obtained.

Soil analysis: Soil samples were collected from both the Aljouf and Qassim regions at a depth of 0–30 cm. The samples were air-dried and passed through a 2-mm sieve. Soil texture was determined using the hydrometer method. A 1:5 soil–water extract was prepared by mixing 100 g of air-dried soil with 500 mL of distilled water, after which the pH and electrical conductivity (EC, mS/cm) were measured using a pH and conductivity meter (Al-Munqedhi *et al*., 2022).

DNA extraction: Genomic DNA was extracted using a modified Cetyltrimethylammonium bromide (CTAB) protocol Khan *et al*., (2007). Briefly, 0.2 g of leaf tissue was ground to a fine powder in liquid nitrogen and homogenized in 700 µL of pre-warmed CTAB extraction buffer. The mixture was incubated at 65°C for 30 minutes and then purified with chloroform: isoamyl alcohol (24:1). DNA was precipitated using chilled isopropanol, collected by centrifugation, and rinsed with 70% ethanol. The purified DNA was then dissolved in TE buffer, quantified with a Nanodrop 8000 spectrophotometer, and preserved for later PCR applications (Alansi *et al.*, 2016).

ISSR amplification: A total of 20 primers were initially screened, of which 16 ISSR primers (Table 1) generated clear and polymorphic banding patterns across and within populations. ISSR-polymerase chain reaction (PCR) amplification was carried out following the protocol of Zietkiewicz *et al*., (1994) using a Thermal Cycler (Applied Biosystem, Singapore). The PCR program consisted of an initial denaturation at 94°C for 5 min, followed by 35 cycles of denaturation at 94°C for 1 min, annealing at primer-specific temperatures for 1 min, and extension at 72°C for 1.30 min. A final extension was performed at 72°C for 5 min. Amplification products (10 µL) were separated on 1.7% agarose gels containing ethidium bromide, alongside a 100 bp DNA ladder (7 µL) as a size marker. Electrophoresis was conducted at 80 V for 180 min in 1X TBE buffer, and the resulting bands were visualized under UV light using a Bio-Rad ChemiDoc MP Imaging System.

Data analysis: For genetic data analysis, the bands produced by ISSR-PCR were scored as (0) and (1). The missing data (faint and unclear bands) were excluded from the analysis. The binary matrix was used to calculate various parameters such as polymorphic information content (PIC), effective multiple ratios (EMR), polymorphic loci (PL), Marker index (MI), and resolving power (RP). The POPGEN 32 software was used to measure the following parameters: observed number of alleles (na), effective number of alleles (ne), Nei's gene diversity (h), number of polymorphic loci (PL),

percentage of polymorphic loci (PPL), and Shannon's information index. To analyze the genetic diversity in subdivided populations, we determined the total genetic diversity (H_t), intrapopulation genetic diversity (H_s), and genetic differentiation coefficient (G_{st}). The amount of gene flow (Nm) between populations was calculated using population differentiation [$(N_m = 0.5\ (1-G_{st})/G_{st}$], according to McDermott & McDonald, 1993. A dendrogram was constructed based on the genetic distance, UPGMA (unweighted pair-group method with arithmetic averages). Analysis of molecular variance (AMOVA) was performed on two levels: within populations, among populations, and also on three levels: within populations, among populations, and among regions, using the GenAlex cross-platform package version 6.1 based on 999 permutations (Alansi *et al.*, 2016). Cluster analysis was performed by PAST 5.

Estimation of genome size in plant samples from both regions

Nuclei extraction: Young leaves derived from seeds cultured on B5 medium were used for nuclei isolation, with the internal standard Stupické (2C = 1.96 pg) applied to estimate the 2C DNA content of *M. forskalii* using MB01 buffer (pH 7.4), which consisted of 2.5 mM Na_2EDTA, 20 mM MOPS, 0.2% (v/v) Triton X-100, 80 mM KCl, 0.7 mM spermine tetrahydrochloride, and 20 mM NaCl, supplemented with freshly prepared antioxidants 1% PVP and 0.5% β-mercaptoethanol to improve nuclei quality (Al-Qurainy *et al.*, 2022). All extraction steps were performed on ice (4°C), where approximately 30 mg of young leaves were finely chopped with a sharp razor blade into 0.3–0.6 mm pieces in a petri dish containing 500 µL of ice-cold MB01 buffer, and the resulting suspension was gently mixed by pipetting and passed through a 20 µm double nylon mesh. The filtered nuclei were then stained with 50 µg/mL propidium iodide (PI, Sigma, St. Louis, MO, USA) for 10 minutes in the dark under refrigerated conditions and kept on ice until analysis.

Genome size estimation: A minimum of 10,000 propidium iodide (PI)-stained nuclei were analyzed using a Beckman Coulter CytoFLEX FC500 flow cytometer at the Central Laboratory of King Saud University. The capillary flow rate was set to medium, and fluorescence was detected using an FL3 filter. PI emission was measured at 585 nm to determine the 2C DNA content of the sample nuclei. The resulting histograms were processed digitally, and the 2C DNA content of the sample was calculated using the formula:

$$\text{2C DNA content of sample} = \frac{\text{(Fluorescence mean intensity of sample)} \times \text{2C DNA content of standard}}{\text{(Fluorescence mean intensity of standard)}}$$

The haploid genome size (in base pairs) was derived using the conversion 1 pg DNA = 978 Mbp. The histograms were further analyzed to distinguish cell cycle phases: G0/G1 (2C), S-phase, and G2/M (4C). The mean fluorescence intensity of the G0/G1 peak was used for 2C DNA content calculations in *M. forskalii*. To ensure precision, the genome size was determined as the average of two technical replicates and three biological replicates, allowing for the calculation of standard error. The haploid genome size (in Mbp) was calculated using the conversion factor 1 pg DNA = 978 Mbp. The fluorescence histograms were deconvoluted into cell cycle phases (G0/G1, S, and G2/M), with the 2C DNA content of *M. forskalii* determined based on the mean fluorescence intensity of the G0/G1 peak.

Identification of phytochemical constituents

Preparation of plant extract: Two grams of the aerial parts of *M. forskalii* from both populations were collected, air-dried in the shade at room temperature for 21 days, and then ground into a fine powder. The powdered material was extracted with 20 mL of methanol and filtered through Whatman No. 1 filter paper, after which the filtrate was concentrated using a rotary evaporator and further dried in a desiccator. The resulting dry extract was weighed, stored in sterile bottles, and kept under refrigeration until further use (El-Amier *et al.*, 2021).

Gas chromatography mass spectrometry (GC-MS) analysis: 1.5 µL was injected via an autosampler injection system of GC-MS 7890B GC system from Agilent Technologies (Santa Clara, CA, USA). The products were identified using the database-integrated software (NIST MS). The identification of the sample components was achieved using Gas Chromatography coupled with a mass selective detector (GC-MS). For the separation of target compounds, a DB-5 MS capillary column from Agilent technologies (30m length x 0.25mm internal diameter, phase thickness 0.25µm) was used with helium as the carrier gas at a flow rate of 1mL/min, inlet temperature 250°C with split mode ratio (50), and oven temperature ranging from 50 to 250°C with a total analysis time of 61 min (The sample was held at 50°C for 1 min, then heated at 4°C min^{-1} to 250°C and maintained for 10 min). The MS detector was set as follows: Acquisition scan type, mass ranging from 40 to 500 g/mol, scan speed 1.56, 8 min solvent delay, and 230°C MS source temperature.

Antibacterial activity of *M. forskalii* extract: For the antibacterial assay, the extract of *M. forskalii* was dissolved in DMSO at a concentration of 100 mg/mL. Bacterial strains, including *Staphylococcus aureus*, *Escherichia coli,* were obtained from the Department of Botany and Microbiology, King Saud University. Luria broth medium was prepared following product instructions by dissolving 25 g of Luria broth and 8 g of agar in 1 L of water, sterilizing, and pouring it into Petri dishes under a laminar flow hood to prevent contamination. For the assay, bacterial cultures were inoculated in 20 mL LB and incubated overnight at 37°C with shaking at 150 rpm. After incubation, OD600 was recorded, and 100 µL of bacterial suspension (10^6 CFU/mL) was added to fresh tubes containing 20 mL LB supplemented with the plant extract, followed by incubation at 37°C for 12 h. The OD600 was re-measured, and 100 µL of each culture was plated on LB agar. Experiments were performed in triplicate .The antibacterial effect was then calculated using the inhibitory formula described by Alfarraj *et al*., (2023).

$$\text{Inhibitory effect (\%)} = (CFU_{control} - CFU_{treatment})/CFU_{control} \times 100\%,$$

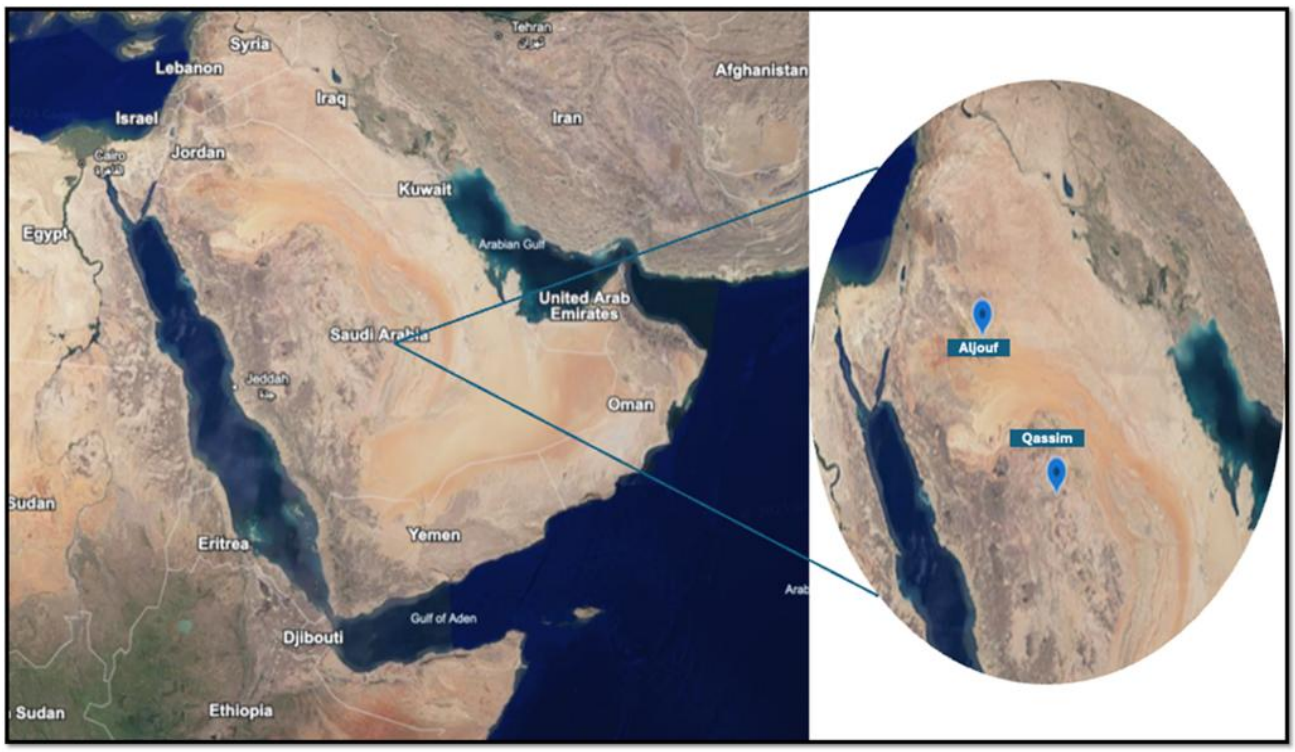

Fig. 1. Map of Saudi Arabia, where the geographical locations of the plant collection sites are indicated (Aljouf, Qassim).

Table. 1. Polymorphism and efficiency parameters of ISSR primers used in the genetic diversity analysis of *Mesembryanthemum forskahlii Hochst. ex Boiss*. Values include primer sequence, annealing temperature (Tm), total number of alleles (Na) , average number of alleles amplified per accession, polymorphic information content (PIC), effective multiplex ratio (EMR), marker index (MI), and resolving power (RP).

No.	Primer	Primer sequence (5'-3')	Annealing temperature (Tm)	Total no. of alleles (Na)	Average no. of Alleles amplified per accession	Polymorphic information content (PIC)	Effective multiplex ratio (EMR)	Marker index (MI)	Resolving power (RP)
1.	842	GA GA GA GA GA GA GA GA YG	50	20	6.652	0.376	6.652	2.501	13.362
2.	858	TGT GTG TGT GTG TGT GRT	46	18	5.811	0.323	5.811	1.879	11.590
3.	JOHN	(AG)7-YC	46	13	4	0.263	4	1.053	7.942
4.	807	AGA GAG AGA GAG AGA GT	47	9	4.855	0.262	4.855	1.274	9.857
5.	836	AGA GAG AGA GAG AGA GYA	50	16	5.695	0.221	5.695	1.260	11.228
6.	840	(GA)8YT	49	10	5.411	0.176	3.788	0.668	10.666
7.	847	CAC ACA CAC ACA CAC ARC	50	23	6.6	0.294	6.6	1.945	13.391
8.	857	ACA CAC ACA CAC ACA CYG	49	22	4.710	0.278	4.710	1.312	7.9
9.	Backy	(CA)7-YC	46	21	5.753	0.312	5.753	1.797	11.507
10.	CHRIC	(CA)7-YG	44	17	4.565	0.273	4.565	1.247	9.130
11.	Manny	(CAC)4-RC	44	28	5.257	0.251	5.318	1.338	10.637
12.	MAO	(CTC)4-RC	46	26	8.117	0.253	7.805	1.976	16.449
13.	OMAR	(GAG)4-RC	45	23	4.260	0.274	4.260	1.168	8.521
14.	S2	CTC-TC-TC-TC-GT-GT-GT-GTG	51	17	5.768	0.355	5.768	2.049	11.536
15.	Terry	(GTG)4-RC [GTG GTG GTG GTG A/G C	45	24	5.940	0.286	5.940	1.703	11.884
16.	Goofy	(GT)7-YG	46	15	3.086	0.272	3.086	0.840	6.173

Antifungal activity of *M. forskalii* extract: The antifungal activity of *M. forskalii* extract was evaluated using three including *Alternaria alternata*, *Aspergillus terreus*, and *Candida tropicalis*, which were obtained from the Department of Botany and Microbiology, King Saud University. For this assay, fungal discs of 2–5 mm in diameter were placed at the center of the plates of potato dextrose agar (PDA) incorporated with plant extract at a concentration of 100 mg/mL and incubated under 27ºC for one week. The inhibitory effects of the plant extracts on radial growth were assessed by measuring fungal colony diameters in both treated and control plates, and the antifungal activity was calculated according to the method described by (Yıldırım *et al.*, 2024):

$$\text{Antifungal activity (\%)} = ((Dc - Ds)/Dc) \times 100$$

"Where Dc is the diameter of growth in the control plate and Ds is the diameter of growth in the plate containing the tested antifungal agent."

Statistical analysis: IBM-SPSS version 26 software was used for statistical analysis of antimicrobial comparison. Two-way ANOVA was subjected to three replicas of data, and various tests were used to detect the significant difference at $p \leq 0.05$.

Result and Discussion

Estimation of genetic variation using ISSR Marker: Genetic diversity is critically important for plant conservation. It represents a fundamental component of biodiversity, and it is a key to enabling plant adaptation to harsh environmental conditions (Salgotra & Chauhan, 2023). Moreover, a multitude of forces on the molecular level, such as point mutations, chromosomal rearrangement, genetic drift, gene flow, and natural selection, can influence the genetic variation among and within populations (Ashango & Abtew, 2025). These mechanisms can shape and influence adaptation and evolutionary trajectories, especially when they act synergistically (Oyarieme *et al.*, 2024). Using 16 ISSR primers, a total of 303 loci were scored across the two studied populations (Aljouf and Qasim), with fragment sizes ranging from 200 to 2000 bp (Fig. 1, Table 2). The majority of loci were polymorphic (PL = 300; PPL = 99.01%), reflecting a high level of genetic variability. Within the two populations, the mean number of observed alleles (na) was 1.9901 ± 0.0992, the effective number of alleles (Ne) was 1.4669 ± 0.3281, Nei's gene diversity (h) was 0.2828 ± 0.1614, and Shannon's information index (I) was 0.4355 ± 0.2082. These values demonstrate considerable allelic richness and genetic variation within the populations.

Partitioning of genetic diversity revealed that intrapopulation diversity (0.2455 ± 0.0198) was comparable to the overall diversity (0.2845 ± 0.0259). The genetic differentiation coefficient (Gst), following Nei (1978), was 0.1369, which falls within the moderate differentiation range (low <0.05; moderate <0.15; high >0.15). This indicates that most genetic variation (~86.3%) resides within populations, while ~13.7% is distributed among populations. A significant level of gene flow was detected (Nm = 3.1532), and since Nm >1, this suggests substantial genetic exchange between the Aljouf and Qassim populations.

Furthermore, Nei's unbiased measures of genetic identity and genetic distance revealed high similarity between the populations. The genetic identity (I) was 0.9015, while the genetic distance (D) was 0.14. These results confirm that the two populations share approximately 90% of their allelic composition, with only moderate genetic differentiation.

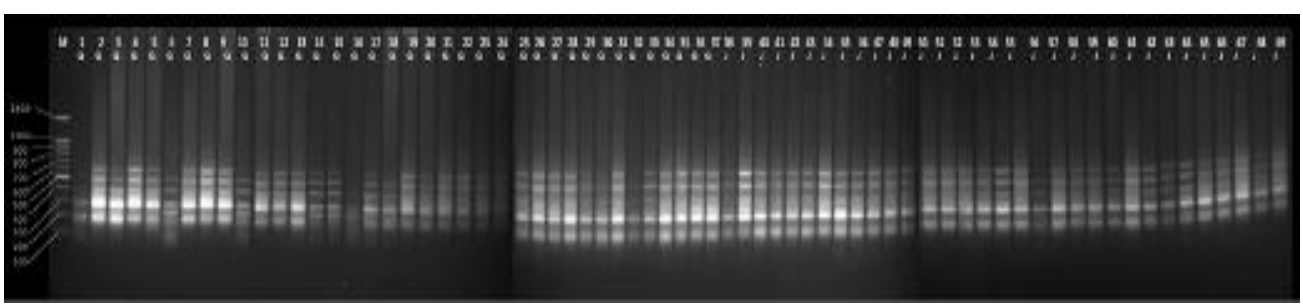

Fig. 2. ISSR profiling of *M. forskalii* populations from Aljouf and Qassim. Gel electrophoresis image showing banding patterns produced by ISSR primer UBC840. Lanes are labeled as follows: Lane M: 100-1500 bp DNA ladder. Lanes 1-37 samples from the Qassim region (Q1-Q37). Lanes 38-69 samples from the Aljouf region (J38-J69).

Table. 2. Genetic diversity parameters of *M. forskalii* populations based on ISSR Markers.

Parameter	Value (mean ± SD)
Observed number of alleles (Na)	1.9901 ± 0.0992
Effective number of alleles (Ne)	1.4669 ± 0.3281
Nei's gene diversity (h)	0.2828 ± 0.1614
Shannon's information index (I)	0.4355 ± 0.2082
Number of polymorphic loci (PL)	300
Percentage of polymorphic loci (PPL)	99.01%
Total genetic diversity (Ht)	0.2845 ± 0.0259
Intra-population diversity (Hs)	0.2455 ± 0.0198
Genetic differentiation (Gst)	0.1369
Gene flow (Nm)	3.1532

The UPGMA dendrogram derived from Nei's unbiased genetic distance separated the two populations into distinct clusters, demonstrating the effectiveness of ISSR markers in distinguishing genetically related groups. The short genetic distance observed further reflects the relatively high gene flow between the Aljouf and Qassim populations. Genetic diversity and population structure are shaped by multiple factors, including geographic distribution, migration, mating systems, and balancing selection (Guo *et al.*, 2021). The patterns revealed in our study may indicate historical gene flow facilitated by natural seed dispersal or cross-pollination. As highlighted by Kling & Ackerly (2021), wind dispersal is another key mechanism influencing genetic patterns and gene flow at the species level. This is particularly relevant for *M. forskalii*, whose small, lightweight seeds are well adapted to wind-mediated dispersal. Human activities may also alter gene flow by reshaping species distribution and dispersal pathways (Crispo *et al.*, 2011). In support of this, Ambaw *et al.*, (2025) reported a high Nm value (5.74) in *Brassica carinata* A. Braun, suggesting extensive gene exchange among subpopulations, attributed to wind- and insect-mediated pollen transfer as well as farmer seed exchange.

The AMOVA analysis at two hierarchical levels revealed that the majority of genetic variance (78%) was partitioned within populations, while only 22% of the variance was distributed among populations (Table 3). These findings are consistent with previous studies that demonstrate the value of

within-population variation exceeding among-population variation. This pattern has been reported in the medicinal plant *Viola canescens,* which showed a high level of genetic variation within populations at 74%, compared to only 26% among populations, and by *Mesembryanthemum* species, where within population variation reached 53% with ISSR and 73% with RAPD markers, against 47% among populations(Kumar & Sharma, 2025; Soliman *et al.*, 2014) . The high proportion of genetic variation within populations suggests that *M. forskalii* may be predominantly outcrossing, similar to the pattern reported for *Ziziphus spina-christ* growing in Saudi Arabia, where genetic variation within the population reached 90% (Alansi *et al.*, 2016). In contrast, the 35 populations within the Oophytum (Aizoaceae) genus located in south Africa exhibited genetic variation within populations (41%) and among populations (42%) than among regions (17%). This pattern is attributed to restricted gene flow, resulting from historical climate shifts and adaptation to fragmented habitats (Schmidt *et al*., 2025). In our study, the observed variation can also be explained by gene flow, which introduces new alleles into the gene pool and homogenizes populations (Oyarieme *et al.*, 2024). This is further supported by the high percentage of polymorphic loci (PPL) and the relatively low genetic differentiation among populations.

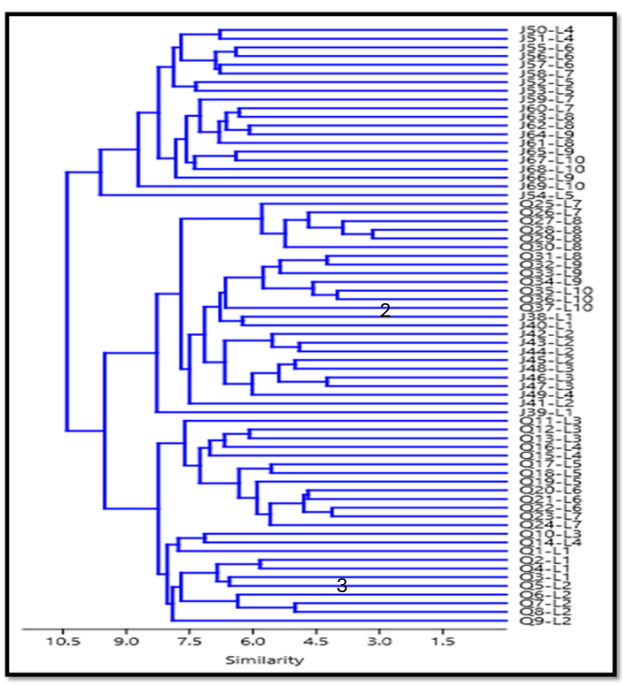

Fig. 3. Dendrogram based on UPGMA analysis of the Dice similarity coefficient among *M. forskalii* populations as determined by Inter-Simple Sequence Repeats (ISSR).

The UPGMA dendrogram based on Dice similarity coefficients (Fig. 3) revealed three major clusters subdivided into six subclusters. The primary split separated the Aljouf and Qassim populations, reflecting the influence of geographic isolation on gene flow, a common feature in wild plant populations (Chai *et al.*, 2024). Similar clustering patterns have been reported in *Quercus petraea*, where historical events and environmental conditions played significant roles in shaping genetic structure (Rebrean *et al.*, 2023). Likewise, Liu *et al.,* (2023) found substantial genetic differentiation among 18 populations of *Cephalotaxus oliveri*, attributed to environmental heterogeneity. Interestingly, the third cluster in our dendrogram comprised individuals from both populations, including samples from Qassim (locations 7, 8, 9, and 10) and Aljouf (locations 1, 2, 3, and 4). The mixed grouping suggests a genetic signal of historical or ongoing gene flow between the regions, despite geographic separation. A similar pattern was reported in *Aloe peglerae* (Asphodelaceae) by Schmidt *et al.,* (2025), where gene flow was facilitated by natural seed dispersal and cross-pollination, contributing to genetic exchange across populations (Andrews, 2010).

The PCoA analysis (Fig. 4) corroborated the UPGMA results, confirming the presence of three main clusters across the studied populations. The ordination plot of ISSR marker data showed a dispersed distribution, with clear but partially overlapping clustering patterns. Aljouf samples were primarily concentrated in the left quadrants, although one outlier exhibited slight separation from the main cluster. In contrast, Al-Qassim samples were mainly localized in the upper right quadrant, displaying a broader spread. The third cluster, situated in the lower right quadrant, comprised samples from both populations, again suggesting ongoing gene flow and supporting the AMOVA results that indicated low genetic differentiation among populations.

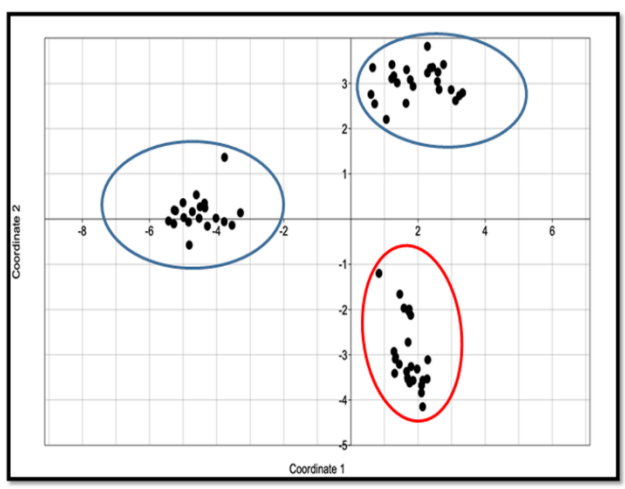

Fig. 4. Two-dimensional plots of Principal Coordinate Analysis (PCoA) indicating the relationship among *M. forskalii* based on ISSR markers.

Genome size estimation of *M. froskhalii* using flow cytometry (FACS): Genome size (GS), or the C-value, represents the total nuclear DNA content of a cell. For more than sixty years, GS has been measured across diverse organisms, with over 7,000 species of embryophytes studied to date (Leitch & Leitch, 2013). Land plants display extraordinary variation, exceeding a 2,400-fold difference in C-values (Pellicer *et al.*, 2018). Genome size estimation is commonly performed using either bioinformatics approaches (e.g., k-mer analysis) or flow cytometry, the method employed in this study.

Despite its broad ecological range, the GS of *Mesembryanthemum forskahlii* has not been previously characterized. Comparative evidence from the Aizoaceae family reveals substantial variability, with values ranging from 0.54 to 6.34 pg (mean = 2.6 pg) (Powell *et al.*, 2020). Our study provides the first estimates of GS for two geographically distinct populations of *M. forskalii* using

flow cytometry. The Aljouf population exhibited a genome size of 0.845 pg, which is slightly less than the Qassim population, 1.059 pg (Fig. 5). These values fall within the known Aizoaceae range (0.54–6.34 pg/2C) and mirror the relatively low GS variation reported in other species of the family despite ecological divergence. The restricted variation observed in *M. forskalii* may result from stabilizing selection, which conserves GS across populations, or from a reliance on phenotypic plasticity rather than genomic restructuring for adaptation (Powell *et al.*, 2020). Gene flow may further homogenize GS between populations, while the species' potential recent range expansion may have limited the time available for divergence (Ellstrand, 2014; Hewitt, 2000). Moreover, the conserved, small genome sizes characteristic of Aizoaceae, including *M. forskalii*, resemble patterns in other recently radiated groups (Pellicer *et al.*, 2018). Geospatially, Aljouf stands at 693 meters above sea level, while Qassim stands at a relatively higher altitude of 795 meters, and they are 572.41 km apart. This altitudinal difference corresponds to a variation in their thermal profile. The temperature in Aljouf ranges from 9.8 to 33.8°C, while in Qassim it exhibits a range of 10 to 45°C. Soil physical properties were listed in Table 4. The physical soil analysis reveals that both Aljouf and Qassim samples are sandy loams in texture. Moreover, both soils are alkaline, with pH values of 8.28 and 8.04, respectively, for Aljouf and Qassim. Furthermore, the electrical conductivity (EC) measurements show a notable difference in salinity, with the Aljouf sample having a lower salinity level (311 µS/cm compared to Qassim (479 µS/cm), suggesting that the second site may pose a risk of salt stress to sensitive plants. The environmental divergence between these two populations, such as temperature, altitude, and soil texture, might be the cause of the slight variation in genome size of *M. forskalii*. Environmental stress can influence GS dynamics, with polyploidization serving as an adaptive expansion mechanism under variable conditions, and genome downsizing conferring energetic efficiency in more stable environments (Sun *et al.*, 2017; Fragata *et al.*, 2019; He *et al.*, 2024; Wang *et al.*, 2021). These processes contribute to divergence within and between populations.

Table. 3. Analysis of molecular variance (AMOVA) for genetic diversity in *M. forskalii* populations.

Source	df	SS	MS	Est. Var.	%
Among Pops	1	404.861	404.861	10.687	22%
Within Pops	67	2551.603	38.084	38.084	78%
Total	68	2956.464		48.771	100%

df: Degrees of freedom, SS: Sum of squares, MS: Mean square, Est. Var.: Estimated variance

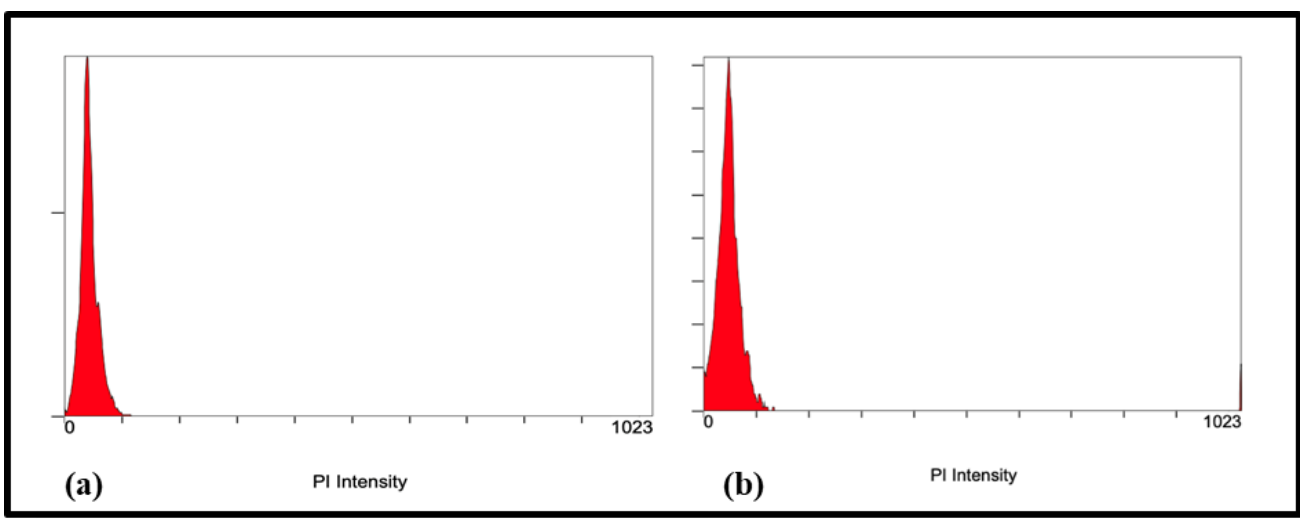

Fig. 5. A flow cytometry histogram of *M. forskalii* from Aljouf (a) Qassim populations (b).

Table. 4. Soil physical properties.

Sample	Sand (%)	Silt (%)	Clay (%)	pH	EC (µS/cm)
Aljouf	84.48	3.43	12.09	8.28	311
Qassim	86.7	1.07	12.23	8.04	479

Phytochemical constituents of *Mesembryanthemum forskahlii Hochst. ex Boiss.* extract: The phytoconstituents identified through GC–MS analysis, along with their documented biological activities, are listed in Table 5. Quantitative evaluation based on peak area percentages revealed distinct regional variations. In the Aljouf extract, **n-**hexadecanoic acid (palmitic acid) was the most abundant compound. Palmitic acid is a long-chain saturated fatty acid and a key precursor in cuticular wax biosynthesis, contributing to the formation of a protective hydrophobic barrier that reduces pathogen invasion and water loss (Purushothaman *et al.*, 2025). Its oxidation derivatives, including various oxylipins, also function as signaling molecules in jasmonic acid-mediated plant defense responses (Kuźniak & Gajewska, 2024).

Table 5. Bioactive compounds of *Mesembryanthemum forskahlii* Hochst. ex Boiss. obtained from the GC-MS spectrum of both regions Aljouf and Qassim.

Compounds	Aljouf		Qassim		Biological activity
	RT	%	RT	%	
Levomenthol	14.152	1.490358	-	-	relieve minor throat irritation.(Wade *et al.*, 2019)
Desulphosinigrin	33.134	0.860817	-	-	have antimicrobial activity (Sosa *et al.*, 2016)
Hexadecanoic acid, methyl ester	36.498	14.95797	-	-	antioxidant, antibacterial, and antifungal activity (Hasan *et al.*, 2019)
n-Hexadecanoic acid	37.638	0.98617	37.772	12.00806	anti-inflammatory and antibacterial activity (Mahmoud *et al.*, 2025)
9,12-Octadecadienoic acid (Z,Z)-, methyl ester	40.433	6.754237	-	-	analgesic, anti-inflammatory, and ulcerogenic activity (Hadi *et al.*, 2016)
9-Octadecenoic acid (Z)-, methyl ester	40.619	9.853518	40.598	2.117233	antimicrobial effect (Javaid *et al.*, 2021),
10-Octadecenoic acid, methyl ester	40.74	1.237567	40.829	1.187969	antibacterial, antifungal, and antioxidant properties, ecrease blood cholesterol (Belakhdar *et al.*, 2015)
11-Octadecenoic acid, methyl ester	40.831	0.792077	41.242	0.606147	Antibacterial, antifungal and antioxidant (Mahmoud *et al.*, 2025), Antidiarrhoeal activity (Shoge & Amusan, 2020)
β-Sitosterol	44.703	0.874113	-	-	anti-inflammatory (Khan *et al.*, 2022), anticancer, hepatoprotective, antioxidant, cardioprotective, and antidiabetic properties (Mahmoud *et al.*, 2025)
γ-Sitosterol	44.801	0.892362	-	-	therapeutic effect on diabetes by reducing hyperglycemia in diabetic-induced rats (Tripathi *et al.*, 2013). anticancer (Sundarraj *et al.*, 2012), antifungal, and antibacterial activities (Rafiq *et al.*, 2025)
Ethyl iso-allocholate	45.077	4.075141	-	-	antioxidant and antidiabetic properties (I *et al.*, 2024).
Oxiraneundecanoic acid, 3-pentyl-, methyl ester, trans-	45.629	1.096593	-	-	antioxidant and anticancer activity (Al-Marzoqi *et al.*, 2016)
cis-11-Eicosenoic acid	49.132	0.331534	-	-	antimicrobial activity (Suresh *et al.*, 2014)
Vitamin E	52.796	3.090059	-	-	ntioxidant and anti-inflammatory(Jiang, 2014)
22-Tricosenoic acid	53.044	1.1238	-	-	antiaxiolytic effects (Selvan & Velavan, 2015).
7,8-Epoxylanostan-11-ol, 3-acetoxy-	54.965	0.913834	-	-	antimicrobial and anti-inflammatory effects (Alqahtani *et al.*, 2020)
9,12,15-Octadecatrienoic acid, 2,3-dihydroxypropyl ester, (Z,Z,Z)-	55.303	2.683948	-	-	anti-inflammatory and CNS depressant activity (Idan *et al.*, 2015).
Oleic acid, eicosyl ester	56.079	0.816251	-	-	insectifuge and to have anti-inflammatory, cancer preventive, hypocholesterolemic (Wyson *et al.*, 2016), and antimicrobial properties (Ashour *et al.*, 2025)
Campesterol	56.435	2.085875	56.667	5.235303	anti-cholesterol, anticarcinogenic, antiangiogenic properties (Javaid *et al.*, 2021) and antimbacterial activities (Mahmoud *et al.*, 2025).
Ergost-5-en-3-ol, (3β)-	56.737	6.787881	-	-	anti-cholesterol, anticarcinogenic, antiangiogenic properties (Javaid *et al.*, 2021) and antimbacterial activities (Mahmoud *et al.*, 2025).
Stigmasterol	58.693	4.139407	58.63	5.614579	antitumor and antidiabetic (Sunday *et al.*, 2025) Anticancer properties (Mahmoud *et al.*, 2025).
Cyclohexanol, 5-methyl-2-(1-methylethyl)-	-	-	14.127	1.18308	antimicrobial, anticancer, antitumor, analgesic, anti-inflammatory, sedative, antifungal, cholesterol-lowering, insecticidal, chemopreventive, and pesticide (Hasan *et al.*, 2019).
Ascaridole epoxide	-	-	18.763	2.824484	anti-inflammatory activity.(Sosa *et al.*, 2016)
Methyl jasmonate	-	-	21.792	0.571755	antioxidant activity (Wang *et al.*, 2009)
3,5-Heptadienal, 2-ethylidene-6-methyl-	-	-	23.503	0.271046	anti-inflammatory, antitumor, and antiviral properties (Altameme *et al.*, 2016).
Cedran-diol, 8S,13-	-	-	28.326	0.395322	antitumor, antimicrobial, and anti-inflammatory properties (Youssef *et al.*, 2023)
Spiro[4.5]decan-7-one, 1,8-dimethyl-8,9-epoxy-4-isopropyl-	-	-	30.217	0.538583	anti-inflammatory properties (Shareef *et al.*, 2016)
Tetradecanoic acid	-	-	32.589	3.650809	(Sosa *et al.*, 2016) anti-inflammatory, antimicrobial, and antispasmodic effects (Sosa *et al.*, 2016)
5-O-Methyl-d-gluconic acid dimethylamide	-	-	36.003	3.53247	antimicrobial and antioxidant activity (Arulmanickam & Chitra, 2020)
Galacto-heptulose	-	-	36.466	2.409748	immunosuppressive effect (Ma'ruf *et al.*, 2022)
Ethanol, 2-(9-octadecenyloxy)-, (Z)-	-	-	41.77	12.69438	has listed as a bioactive componds in study on antibacterial activity of *Shuteria involucrata* extracts by (Senthamizh Selvan & Isaiah, 2018)
Cholestan-3-ol, 2-methylene-, (3β,5α)-	-	-	43.404	0.791965	has anti-inflammatory and cytotoxic activities as reported in study of (Altameme *et al.*, 2016).
Ethyl iso-allocholate	-	-	45.953	1.121394	antimicrobial activity (Malathi *et al.*, 2017)
Corynan-17-ol, 18,19-didehydro-10-methoxy-, acetate (ester)	-	-	51.232	0.316544	anti-diarrhoeal activity (Hussein *et al.*, 2016)
Lupeol	-	-	53.152	33.33793	Anticancer, antiprotozoal, chemopreventive and anti-inflammatory properties (Altameme *et al.*, 2016).

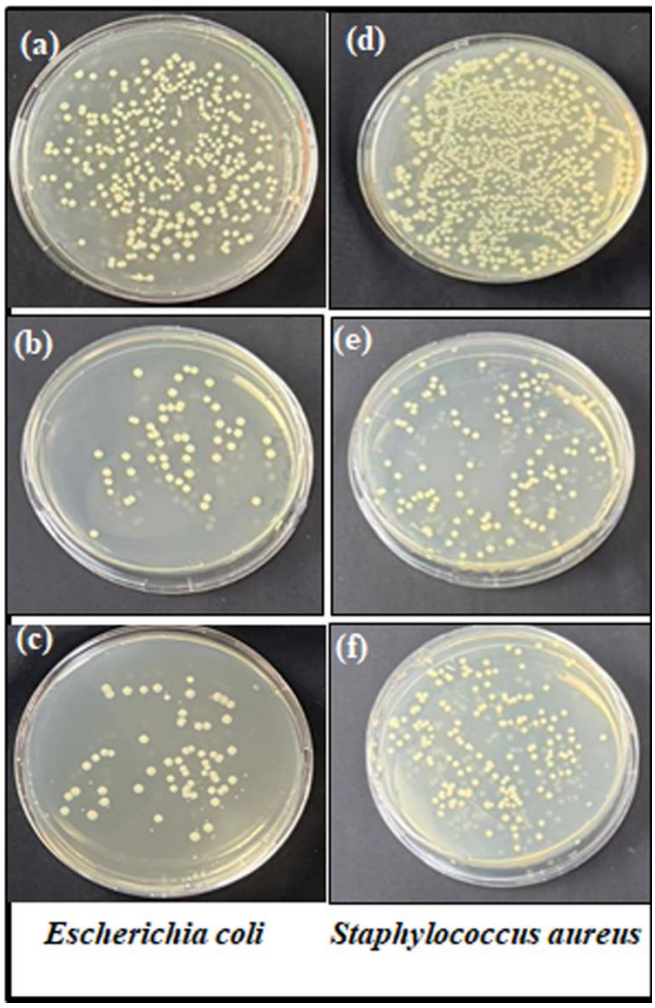

Fig. 6. Antibacterial activity of *M. forskalii* extracts from Aljouf and Qassim regions against bacterial strains *Escherichia coli* (a: control) (b: Aljouf) (c: Qassim) and *Staphylococcus aureus* (d: control) (e: Aljouf) (f: Qassim), after 24h of incubation at 37°C.

Previous studies have further demonstrated the biocidal activity of palmitic acid, such as its toxic effect against fire ants in *Capsicum pubescens* (Coyotl-Pérez *et al*., 2025). In addition, palmitic acid is known for its anti-inflammatory, antioxidant, and broad-spectrum antibacterial properties (Atawodi *et al.,* 2025; Mahmoud *et al.,* 2025). In the present study, n-hexadecanoic acid accounted for 14.96% of the total peak area in the Aljouf extract, compared to 12.01% in the Qassim extract. Similarly, palmitic acid has been reported as the dominant saturated fatty acid in four Red Sea halophytic species from Saudi Arabia, *Anabasis ehrenbergii*, *Suaeda aegyptiaca*, *Suaeda monoica*, and *Zygophyllum album,* with concentrations ranging from 23.94% to 49.49% (Hawas *et al*., 2022).

Similarly, 9,12-Octadecadienoic acid (Z, Z)-methyl ester, which exhibits analgesic, anti-inflammatory, and ulcerogenic activity (Hadi *et al.*, 2016), was more dominant in Aljouf (6.75%) than in Qassim (1.20%). 9-Octadecenoic acid (Z)-methyl ester, recognized for its antimicrobial potential, was also higher in Aljouf (9.85%) (Javaid *et al.*, 2021). The Qassim extract was dominated by Lupeol, accounting for 33.33% of the total composition. Lupeol is a multifunctional triterpenoid with anticancer, antiprotozoal, chemopreventive, and anti-inflammatory activities (Altameme *et al.*, 2016). In plants, lupeol serves as a defense scaffold, with its glycosylated derivatives directly impairing herbivore performance and contributing to the plant's broader chemical defense (Yang *et al.,* 2024*)*. Beyond its antiherbivore effects, lupeol metabolite in plants contributes to adaptation to broader stresses through antimicrobial activity and phytohormone modulation (Li *et al*., 2023). It has also been widely documented in *Tamarindus indica*, *Allanblackia monticola*, *Emblica officinalis*, elm bark, and olive fruit, where it shows significant therapeutic potential in treating cancer, diabetes, and cardiovascular, liver, kidney, and skin disorders (Dalimunthe *et al.*, 2024). Campesterol, known for its anti-cholesterol, anticarcinogenic, antiangiogenic, and antibacterial effects, was present at 2.09% in Aljouf (Javaid *et al.*, 2021; Mahmoud *et al.*, 2025). In Qasim, the corresponding sterol was identified as Ergost-5-en-3-ol, (3β)-, at 6.78% and 5.24%. Stigmasterol, another phytosterol with reported antitumor, antidiabetic, and anticancer activities, was found at 4.14% in Aljouf and 5.61% in Qasim (Mahmoud *et al.*, 2025). The occurrence of Campesterol and Stigmasterol supports the traditional medicinal uses of *Mesembryanthemum forskahlii*, including cholesterol-lowering effects and antifungal activities against hair pathogens (Al Faris *et al*., 2011; Bilel *et al.*, 2020).

Overall, GC–MS profiling of methanolic extracts from *M. forskalii* collected in Aljouf and Qassim revealed distinct regional variation in phytochemical composition. These differences are likely shaped by environmental heterogeneity, including soil and climatic conditions (Mansinhos *et al.*, 2024). Similar findings were reported by Zamani *et al.,* (2025), who showed that environmental factors strongly influenced the secondary metabolite profiles of *Stachys lavandulifolia* in Iran. Likewise, Ogundola *et al.,* (2022) demonstrated that soil texture significantly alters the phytochemical and antioxidant composition of *Solanum nigrum*. Thus, the phytochemical disparities observed between the Aljouf and Qassim populations of *M. forskalii* can be attributed to their distinct environmental contexts, which play a decisive role in shaping secondary metabolite diversity.

Antibacterial activity of *Mesembryanthemum forskahlii* Hochst. ex Boiss. leaves extracts: In recent years, there has been growing interest in using natural and organic resources for applications such as food preservation and medicinal therapies. Many studies have reported the antimicrobial activity of plant extracts against pathogenic bacteria and fungi (El-Amier *et al.*, 2021). The Aizoaceae family is well known for its wide range of biological activities, including antibacterial, antifungal, anticancer, antioxidant, and anti-inflammatory properties (Ibtissem *et al.*, 2010). Within this family, species of the *Mesembryanthemum* genus have demonstrated particularly strong antimicrobial, antioxidant, antiviral, and anticarcinogenic effects (Abdel Gawad *et al.*, 2018).

In the present study, methanolic extracts of *Mesembryanthemum forskahlii* from two populations were evaluated against Gram-negative *Escherichia coli* and Gram-positive *Staphylococcus aureus* (Fig. 6). The extracts showed strong antibacterial activity, with 70.28% inhibition against *E. coli*. This result is consistent with Aabed & Mohammed (2021), who observed inhibition

(94%) using silver nanoparticle (AgNP) derivatives of seed extracts against *E. coli*. Furthermore, in our study, the inhibition of *Staphylococcus aureus* reached 55.66% which is aligns with El-Amier *et al.* (2021), who reported that although *M. forskahlii* ethanolic extract showed a broad inhibition spectrum (50%), it exhibited particularly low efficacy against *S. aureus*. The lower inhibition against *S. aureus* compared to *E. coli* may be related to the structural resilience of Gram-positive bacteria, particularly their thick peptidoglycan cell wall (Al-Otaibi & Al-Motwaa, 2025). When comparing the two populations, Aljouf extracts recorded higher inhibition against both bacteria (*E. coli*: 74.04%; *S. aureus*: 58.74%) than Qassim extracts (*E. coli*: 66.52%; *S. aureus*: 52.57%). The higher inhibition observed in the Aljouf extract is most likely attributed to its greater concentration of compounds with antimicrobial activities, such as n-Hexadecanoic acid and 9-Octadecenoic acid (Z)-, methyl ester.

Antifungal activity of *Mesembryanthemum forskahlii* Hochst. ex Boiss. leaves extracts: The antifungal activity of the extracts was also examined against *Alternaria alternata*, *Aspergillus terreus*, and *Candida tropicalis* (Fig. 7). The strongest effect was observed against *A. alternata* (95% inhibition), while moderate inhibition was recorded for *A. terreus* (71%) and *C. tropicalis* (65%). These results are consistent with Bilel *et al*. (2019), who reported similar antifungal effects using plant seed extracts, as they inhibited fungal growth by 88% against *Penicillium chrysogenum* and *Aspergillus fumigatus*, 85% against *A. flavus* and *A. carneus*, and between 60-75% against other fungi. A similar study, Hussain *et al*., (2025) found that ethanolic extracts from the halophyte *Zilla spinosa* showed significant antifungal activity against *Candida albicans* (10.33 mm) using the agar well diffusion method. A population-based comparison revealed stronger inhibition from the Aljouf extract against *A. terreus* (76%) compared with the Qassim extract (66.8%), which can also be linked to the presence of a high amount of n-Hexadecanoic acid (palmitic acid) and other constituents with antifungal function. For *A. alternata*, both extracts demonstrated similar inhibition levels (Aljouf: 95.8%; Qassim: 95%). Overall, the findings confirm that *M. forskalii* extracts possess broad-spectrum antimicrobial properties, with antibacterial and antifungal activity varying between populations, likely due to environmental differences.

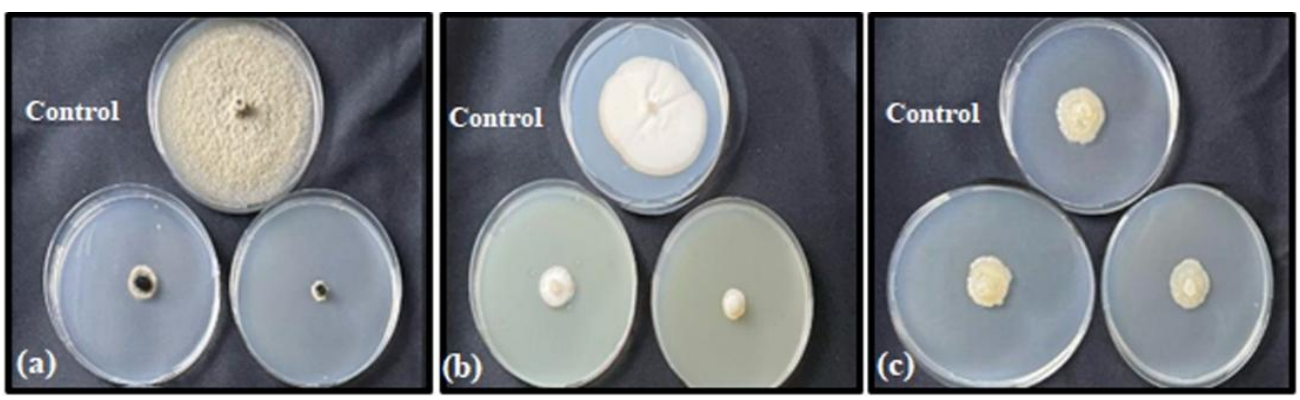

Fig. 7. Antifungal activity of of *M. forskalii* extracts from Aljouf (left plates) and Qassim (right plates) regions against *Alternaria alternata* (a), *Aspergillus terreus* (b), and *Candida tropicalis* (c), compared to an untreated control (top plates), after 8 days of incubation at 27°C.

Conclusion

This study provides the first comprehensive assessment of genetic diversity, genome size variation, phytochemical composition, and antimicrobial activity of *Mesembryanthemum forskahlii* from Aljouf and Qassim regions of Saudi Arabia. The high percentage of polymorphic loci and AMOVA results revealed that most genetic variation resides within populations, supported by moderate genetic differentiation and substantial gene flow. Genome size estimates showed conserved yet regionally distinct values, suggesting genomic stability despite environmental divergence. GC–MS profiling highlighted clear differences in secondary metabolite composition between populations, with Aljouf extracts enriched in bioactive compounds such as n-Hexadecanoic acid, and Qassim extracts dominated by triterpenoids such as Lupeol. Antimicrobial assays demonstrated broad-spectrum activity, with particularly strong inhibition against *E. coli* and *A. alternata*, confirming the pharmacological potential of this species. Overall, the findings underscore the adaptive capacity of *M. forskalii*, its ecological resilience, and its promise as a source of natural bioactive compounds, while also emphasizing the importance of conserving its genetic resources for future medicinal and biotechnological applications.

Author Contributions: Conceptualization, A.Z.A. and A.M.A.M.; methodology, A.Z.A, S.K, and N.S.A.; investigation, A.Z.A and M.N, A. M. S; results, A.Z.A , A. Z.G, S.K; analysis, A.Z.A, A. Z.G; writing, original draft preparation, A.Z.A, and M.T; writing, review and editing, A.Z.A, and M.T., and F.A.-Q; supervised the experiment, F.A.-Q. and A.A.-H. All authors have read and agreed to the published version of the manuscript.

Conflicts of Interest: The authors declare no conflict of interest.

Acknowledgments: The authors extend their appreciation to the Ongoing Research Funding program (ORF-2026-219), King Saud University, Riyadh, Saudi Arabia.

References

Aabed, K. and A.E. Mohammed. 2021. Phytoproduct, arabic gum and opophytum forsskalii seeds for bio-fabrication of silver nanoparticles: Antimicrobial and cytotoxic capabilities. *Nanomaterials*, 11(10): 2573.

Abd El-Raouf, H.S. 2021. Taxonomic significance of leaves in family aizoaceae. *Saudi J. Biol. Sci.,* 28(1): 512-522.

Abdel gawad, A.M., S.A. Tawab, S.S. Sobieh and D.M. Fahmy. 2018. Cytological and phytochemical studies on mesembryanthemum nodiflorum l. *JSRS*, 35(part 1): 237-249.

Abdel-Farid, I.B., U.A. Mahalel, M. Jahangir, H.A. Elgebaly and S.A. El-Naggar. 2016. Metabolomic profiling and antioxidant activity of opophytum forsskalii. *AUSEJ*, -1 6(3837): 268.

Abdel-Hamid, A.M., M. Ibrahim and G.S. Alnusairi. 2021. Comparison of egyptian and saudi mesembryanthemum forskalii hochst. Ex boiss. As an unconventional alternative protein of wheat and barley. *IJEB*, 59(03): 194-201.

Al Faris, N.A., Z.A. Al Othman and D. Ahmad. 2011. Effects of mesembrrybryanthemum forsskalei hochst seeds in lowering glucose/lipid profile in streptozotocin-induced diabetic rats. *JFST,* 48(5): 616-621.

Al-Jassir, M.S., A.I. Mustafa and M. Nawawy. 1995. Studies on samh seeds (mesembryanthemum forsskalei hochst) growing in saudi arabia: 2: Chemical composition and microflora of samh seeds. *Plant Foods Hum. Nutr.,* 48(3): 185-192.

Al-Marzoqi, A., M. Hadi and I. Hameed. 2016. Determination of metabolites products by cassia angustifolia and evaluate antimicobial activity. *J. Pharmacog. Phytother*, 8: 25-48. DOI 10.5897/JPP2015.0367.

Al-Munqedhi, M. Bander, Mohamed A. El-Sheikh and Ahmed H. Alfarhan. 2022. Climate change and hydrological regime in arid lands: Impacts of dams on the plant diversity, vegetation structure and soil in Saudi Arabia. *Saudi J. Biol. Sci.*, 29(5): 3194-206. https://doi.org/10.1016/j.sjbs.2022.01.043.

Al-Otaibi, W.A. and S.M. Al-Motwaa. 2025. A systematic exploration of the nutritional benefits and therapeutic potential of mesembryanthemum forsskalii. *Int. J. Food Sci. Technol.,* 60(1): vvae092. https://doi.org/10.1093/ijfood/vvae092.

AL-Qahiz, N.M. 2009. The impact of samh seeds on blood parameters of experimental animals. *PJN*., 8(6): 872-876.

Al-Qurainy, F., M. Tarroum, S. Khan, M .Nadeem, A.R.Z. Gaafar, S. Alansi and N.S. Alfarraj. 2022. Genome estimation and phytochemical compound identification in the leaves and callus of abrus precatorius: A locally endangered plant from the flora of saudi arabia. *Plants*, 11(4): 567.

Alansi ,S., M. Tarroum, F. Al-Qurainy, S. Khan and M. Nadeem. 2016. Use of issr markers to assess the genetic diversity in wild medicinal ziziphus spina-christi (l.) willd. Collected from different regions of saudi arabia. *Biotechnol. Biotechnol. Equipt*, 30(5): 942-947.

Alderaywsh, F., M.A. Osman, F.Y. Al-Juhaimi, M.A. Gassem, S.A. Al-Maiman, O.Q. Adiamo, M.M. Özcan and I.A.M. Ahmed. 2019. Effect of traditional processing on the nutritional quality and in vivo biological value of samh (mesembryanthemum forsskalei hochst) flour. *J. Oleo Sci.,* 68(10): 1033-1040.

Alfarraj, N.S., M. Tarroum, F. Al-Qurainy, M. Nadeem, S. Khan, A.M. Salih, H.O. Shaikhaldein, A. Al-Hashimi, S. Alansi and K. Perveen. 2023. Biosynthesis of silver nanoparticles and exploring their potential of reducing the contamination of the *In vitro* culture media and inducing the callus growth of rumex nervosus explants. *Molecules*, 28(9): 3666.

Alqahtani, S.S., H.A. Makeen, S.J. Menachery and S.S. Moni. 2020. Documentation of bioactive principles of the flower from caralluma retrospiciens (ehrenb) and *In vitro* antibacterial activity–part b. *Arab.J. Chem.,* 13(10): 7370-7377.

Altameme, H., I. Hameed and S. Idan. 2016. Artemisia annua: Biochemical products analysis of methanolic aerial parts extract and anti-microbial capacity. *RJPBCS*, 7: 1843-1868.

Ambaw, Y.D., A.G. Abitea and T.M. Olango. 2025. Genetic diversity and population structure in ethiopian mustard (*Brassica carinata* a. Braun) revealed by high-density dartseq snp genotyping. *BMC Genom.*, 26(1): 354.

Andrews, C.A. 2010. Natural selection, genetic drift, and gene flow do not act in isolation in natural populations. *Nat. Educ. Know.* pp: 5.

Arena, R., S. Manuguerra, E. Collins, A. Mahdhi, G. Renda, C.M. Messina and A. Santulli. 2020. Antioxidant properties of a supercritical fluid extract of the halophyte mesembryanthemum nodiflorum l. From sicilian coasts: Nutraceutical and cosmeceutical applications. *Appl. Sci.*, 10(7): 2374.

Arivarasu, L. 2023. *In vitro* antioxidant potential of beta-sitosterol: A Preface. NLM.Cureus;15(9): e45617. doi: 10.7759/cureus. 45617.

Arulmanickam, P .and T. Chitra, 2020. Preliminary and secondary phytochemistry of the suicidal plant *Cleistanthus collinus* (Roxb.). *AJMS,* 8(2): 2348-7186.

Ashango, Z. and W.G. Abtew. 2025. Impacts of evolutionary forces on allele and genotype frequency of organisms. *Preprints.org*. doi: 10.20944/preprints202506.0510.v1.

Ashour, M., F.S. Ali, A. Mamoon, M.M. Mabrouk, A.I. Mansour, A.F. Abdelhamid, A.T. Mansour, E. Mohamed and M. Elshobary. 2025. A novel coelastrella tenuitheca isolate enhances growth, immunity, and gene expression in whiteleg shrimp. *Aquac. Nutr,* 2025(1): 4019255.

Atawodi, J.C., J.L. Achika, S.E. Atawodi and R.G.O. Ayo. 2025. Phytochemical composition, antioxidant activity and antimicrobial efficacy of ethyl acetate extract-derived Fraction (FE1) from *Ficus exasperata* Vahl Leaf. *PRENAP,* 7*:* 100213. https://doi.org/10.1016/j.prenap.2025.100213

Awabdeh, S.A., H.M. Asoufi, K.M. Tawarah, K.M. Abulaila and S.S. Al-Nsour. 2022. Chemical profiling analysis of mesembryanthemum (opophytum) forsskalii hochst. Ex boiss in jordan. *Adv. Environ. Biol*, 16: 1-4.

Belakhdar, G., A. Benjouad and E.L.H. Abdennebi. 2015. Determination of some bioactive chemical constituents from thesium humile vahl.. *J. Mater. Environ. Sci*., 6: 2778-2783.

Bilel, H., M.A. Elsherif and S.M.N. Moustafa. 2020. Seeds oil extract of mesembryanthemum forsskalii from Aljouf, Saudi Arabia: Chemical composition, dpph radical scavenging and antifungal activities. *OCL*, 27: 10.

Chai, M.W., H.P. Lu, Y.T. Tseng and P.C. Liao. 2024. Maintenance of species boundaries amid hybridization in two island gingers with similar ecological niches. *Evolution*, 78(3): 526-538.

Coyotl-Pérez, W. A., Y.L. Ángeles-López, S. Luna-Suárez, F.de.F. Rosas-Cárdenas and N. Villa-Ruano. 2025. Volatilomics of *Capsicum pubescens* plants infested by *Solenopsis geminata*: unraveling the role of oleic and palmitic acids in plant-fire ant interaction. *Chem. Biodiv.*, 22(5): e202402380.

Crispo, E., J.S. Moore, J.A. Lee-Yaw, S.M. Gray and B.C. Haller. 2011. Broken barriers: Human-induced changes to gene flow and introgression in animals: An examination of the ways in which humans increase genetic exchange among populations and species and the consequences for biodiversity. *BioEssays*, 33(7): 508-518.

Dalimunthe, A., M.C. Gunawan, Z. Dhiya Utari, M.R. Dinata, P. Halim, N. Estherina S. Pakpahan, A.I. Sitohang, M.A. Sukarno, Yuandani, Y. Harahap, E.P. Setyowati, M.N. Park, S.D. Yusoff, S. Zainalabidin, A.T. Prananda, M.K. Mahadi, B. Kim, U. Harahap and R.A. Syahputra. 2024. In-depth analysis of lupeol: Delving into the diverse pharmacological profile. *Front. Pharm.*, Volume 15 - 2024.

El-Amier, Y., S. Alghanem, O. Al-Hadithy, A. Fahmy and M. El-Zayat. 2021. Phytochemical analysis and biological activities of three wild mesembryanthemum species growing in heterogeneous habitats. *J. Phytol,* 1-8.

Ellstrand, N.C. 2014. Is gene flow the most important evolutionary force in plants. *Amer. J. Bot*, 101(5): 737-753.

Foudah, A.I., F.K. Aloneizi, M.H. Alqarni, A. Alam, M.A. Salkini, H.M. Abubaker and H.S. Yusufoglu. 2022. Potential active constituents from *Opophytum forsskalii* (Hochst. Ex Boiss.) Ne Br against experimental gastric lesions in rats. *Pharmaceuticals*, 15(9): 1089, https://doi.org/10.3390/ph15091089.

Fragata, I., A. Blanckaert, M.A. Dias Louro, D.A. Liberles and C. Bank. 2019. Evolution in the light of fitness landscape theory. *Trends Ecol. Evol.,* 34(1): 69-82.

Guo, B., X. Hao, L. Han, Y. Zhai, S. Zhou, S. Chen, D. Ren and X. An. 2021. Unraveling the genetic diversity and structure of quercus liaotungensis population through analysis of microsatellite markers. *Peer J.*, 9: e1.0922

Hadi, M.Y., G.J. Mohammed and I.H. Hameed. 2016. Analysis of bioactive chemical compounds of *Nigella sativa* using gas chromatography-mass spectrometry. *J. Pharmacog. Phytother,* 8(2): 8-24.

Hasan, M.M., M.R. Al Mahmud and M.G. Isla . 2019. GC-MS analysis of bio-active compounds in ethanol extract of *Putranjiva roxburghii* wall. Fruit peel. *Phcog J.*, 11(1): 146-149.

Hawas, U.W., L.T.A. El-Kassem, F.M. Shaher, R. Al-Farawati and M. Ghandourah. 2022. Phytochemical Compositions of Some Red Sea Halophyte Plants with Antioxidant and Anticancer Potentials. *Molecules*, 27(11): 3415.

He, B., W. Liu, J. Li, S. Xiong, J. Jia, Q. Lin, H. Liu and P. Cui. 2024. Evolution of plant genome size and composition. *GPB***,** 22(5): qzae078.

Hewitt, Godfrey. 2000. The genetic legacy of the Quaternary ice ages. *Nature*, 405(6789): pp. 907-913.

Hussain, A., A. Mouhaddach, I. Khalid, T. Kausar, M. Bouhrim, A.A. Shahat, O.M. Noman, B. Eto, S. Yaqub, R. Arshad, H. Farooq, N. Firdous and M. Bilal. 2025. Nutritional, bioactive, and antimicrobial analysis of powders and ethanolic extracts of three important halophyte plants (*Anabasis articulata*, *Lycium shawii*, and *Zilla spinosa*), and their application in bakery product. *Front. Sustain. Food Syst.*, 9: 1509423.

Hussein, H.M., I.H. Hameed and J.M. Ubaid. 2016. Analysis of the secondary metabolite products of ammi majus and evaluation anti-insect activity. *IJPPR,* 8(8): 1192-1189.

I, J., V. Priya V and S. Jayaraman. 2024. Antidiabetic and antioxidant potential of ethyl iso-allocholate is mediated through insulin receptor/irs-1/akt/glut 4 mediated pathways: *In vitro* and *In silico* mechanisms. *TIJPH,* doi:10.21522/TIJPH.2013.SE.24.03.Art015.

Ibtissem, B., M. Imen and S. Souad. 2010. Dosage of 2, 6-bis (1.1-dimethylethyl)-4-methylphenol (bht) in the plant extract mesembryanthemum crystallinum. *BioMed. Res. Int.*, 2010(1): 142486.

Idan, S.A., A.H. Al-Marzoqi and I.H. Hameed. 2015. Spectral analysis and anti-bacterial activity of methanolic fruit extract of citrullus colocynthis using gas chromatography-mass spectrometry. *Afr. J. Biotechnol.*, 14(46): 3131-3158.

Javaid, A., M.F. Ferdosi, I.H. Khan, A. Shoaib, M.S. Hafiz and M.A.U. Hassan. 2021. Biochemical analysis of flowers of vinca major, a medicinal weed plant of hilly areas of pakistan. *Pak. J. Weed Sci. Res.*, 27(4): 537.

Jiang, Q. 2014. Natural forms of vitamin e: Metabolism, antioxidant, and anti-inflammatory activities and their role in disease prevention and therapy. *Free Radic.Biol. Med.*, 72: 76-90.

Khan, S., M.I. Qureshi, T. Alam and M. Abdin. 2007. Protocol for isolation of genomic DNA from dry and fresh roots of medicinal plants suitable for rapd and restriction digestion. *Afr. J. Biotechnol*, 6(3): 175.

Khan, Z., N. Nath, A. Rauf, T.B. Emran, S. Mitra, F. Islam, D. Chandran, J. Barua, M.U. Khandaker and A.M. Idris. 2022. Multifunctional roles and pharmacological potential of β-sitosterol: Emerging evidence toward clinical applications. *Chem. Biol. Interact,* 365: 110117.

Kling, M.M. and D.D. Ackerly. 2021. Global wind patterns shape genetic differentiation, asymmetric gene flow, and genetic diversity in trees. *PNAS,* 118(17): e2017317118.

Kumar, R. and V. Sharma. 2025. Elucidation of genetic diversity and population structure in medicinal plant *Viola canescens* from North Western Himalayas. *JARMAP*, 48: 100657.

Kuźniak, E. and E. Gajewska. 2024. Lipids and lipid-mediated signaling in plant–pathogen interactions. *Int. J. Mol. Sci.*, 25(13): 7255.

Labarrere, B., A. Prinzing, T. Dorey, E. Chesneau and F. Hennion. 2019. Variations of secondary metabolites among natural populations of sub-antarctic ranunculus species suggest functional redundancy and versatility. *Plants*, 8(7): 234.

Leitch, I.J. and A.R. Leitch. 2013. Genome size diversity and evolution in land plants. In: Plant genome diversity volume 2: Physical structure, behaviour and evolution of plant genomes. (Eds.): Greilhuber, J., J. Dolezel and J.F. Wendel. *Springer Vienna, Vienna*: pp: 307-322.

Li, C., W. Zha, W. Li, J. Wang and A. You. 2023. Advances in the biosynthesis of terpenoids and their ecological functions in plant resistance. *Int. J. Mol. Sci.,* 24(14): 11561.

Liu, H., Z. Wang, Y. Zhang, M. Li, T. Wang and Y. Su. 2023. Geographic isolation and environmental heterogeneity contribute to genetic differentiation in cephalotaxus oliveri. *Ecol. Evol*., 13(3): e9869.

Ma'ruf, N.Q., E. Hotmian, A.D. Tania, I. Antasionasti, Fatimawali and T.E. Tallei. 2022. In silico analysis of the interactions of *Clitoria ternatea* (L.) bioactive compounds against multiple immunomodulatory receptors. *In: AIP Conf. Proc,. AIP Publishing* LLC: pp: 070006.

Mahmoud, A.D., S.S. Al-Rawi and H.A. Hama. 2025. Traditional uses, bioactive compounds and pharmacological uses of *Vitex doniana* sweet: A review. *Ethnobot. Res. Appl.,* 30: 1-130.

Malathi, K., A. Anbarasu and S. Ramaiah. 2017. Ethyl iso-allocholate from a medicinal rice karungkavuni inhibits dihydropteroate synthase in escherichia coli: A molecular docking and dynamics study. *Ind. J. Pharm. Sci.*, 78(6): 780-788.

Mallon, L. 2012. Mesembryanthemum cristallinum-new crop summary & recommendations. *Horticultural Science, 5051: Plant Production II. University of Minnesota*.

Mansinhos, I., S. Gonçalves and A. Romano. 2024. How climate change-related abiotic factors affect the production of industrial valuable compounds in lamiaceae plant species: A review. *Front. Plant Sci.*, 15: 1370810.

McDermott, J.M. and B.A. McDonald. 1993. Gene flow in plant pathosystems. *Annu. Rev. Phytopathol*., 31: 353-73.

Mint Abdelaziz, S., L. Medraoui, M. Alami, O. Pakhrou, M. Makkaoui, A. Ould Mohamed Salem Boukhary and A. Filali-Maltouf. 2020. Inter simple sequence repeat markers to assess genetic diversity of the desert date (*Balanites aegyptiaca* Del.) for sahelian ecosystem restoration. *Sci. Rep.*, 10(1): 14948.

Mohammed, B.M., I.A. Mohamed Ahmed, G.M. Alshammari, A.A. Qasem, A.E.A. Yagoub, M.A. Ahmed, A.A. Abdo and M.A . Yahya. 2023. The effect of germination and fermentation on the physicochemical, nutritional, and functional quality attributes of samh seeds. *Foods*, 12(22): 4133.

Ogundola, A.F., C. Bvenura, A.F. Ehigie and A.J. Afolayan. 2022. Effects of soil types on phytochemical constituents and antioxidant properties of solanum nigrum. *S. Afr. J. Bot.*, 151: 325-333.

Ogwu, M.C., S.C. Izah and M.T. Joshua. 2025. Ecological and environmental determinants of phytochemical variability in forest trees. *Phytochem. Rev.*, 1-29.

Oyarieme, H., J. Otiti and O. Obros. 2024. A review on genetic variations within and between populations: A population genetic perspective. *Amer. Res. J. Biosci.,* 9: 01-10 Pages. doi 10.21694/2379-7959.24001.

Pellicer, J., O. Hidalgo, S. Dodsworth and I.J. Leitch. 2018. Genome size diversity and its impact on the evolution of land plants. *Gene*s, 9(2): 88.

Powell, R.F., L. Pulido Suarez, A.R. Magee, J.S. Boatwright, M.V. Kapralov and A.J. Young. 2020. Genome size variation and endopolyploidy in the diverse succulent plant family aizoaceae. *Bot. J. Linn. Soc*, 194(1): 47-68.

Purushothaman, R., G. Vishnuram and T. Ramanathan. 2025. Antiinflammatory efficacy of n-Hexadecanoic acid from a mangrove plant *Excoecaria agallocha* L. through in silico, *In vitro* and *In vivo*. *PRENAP*, 7: 100203.

Rafiq, M., A. Shoaib, A. Javaid, S. Perveen, U.A. Hafiz and C. Cheng. 2025. Phytochemical profile of stem extract of *Carthamus oxycantha* and identification of herbicidal and antimicrobial constituents. *Plant Prot. Sci.,* 61(2): 172.

Rebrean, F.A., A. Fustos, K. Szabo, T.-T. Lisandru, M.S. Rebrean, M.I. Varga and D. Pamfil. 2023. Genetic diversity and structure of *Quercus petraea* (matt.) liebl. Populations in central and northern romania revealed by srap markers. *Diversity*, 15(10): 1093.

Salgotra, R.K. and B.S. Chauhan. 2023. Genetic diversity, conservation, and utilization of plant genetic resources. *Genes*, 14(1): 174.

Schmidt, S. A., U. Schmiedel, F. Carstens, A.L. Rau and B. Rudolph-Bartsch. 2025. Diversity on a small scale: Phylogeography of the locally endemic dwarf succulent genus *Oophytum* (Aizoaceae) in the Knersvlakte of South Africa. *Ann. Bot.*, 135(4): 735-756.

Schmidt, X., N. Barker and A. Frisby. 2025. Assessment of the genetic diversity of the critically endangered aloe peglerae schönland (asphodelaceae) by means of inter-simple sequence repeat (ISSR) markers. *S. Afr. J. Bot.,* doi:10.1016/j.sajb.20.25.08.042

Selvan, P.S. and S. Velavan. 2015. Analysis of bioactive compounds in methanol extract of cissus vitiginea leaf using gc-ms. *Rasayan J. Chem.*, 8(4): 443.

Senthamizh Selvan, N. and S. Isaiah. 2018. Gc-ms analysis and antibacterial activity of different solvent extracts of shuteria involucrata. *J. Phytopharm*, 7: 116-120.

Shareef, H.K., H.J. Muhammed, H.M. Hussein and I.H. Hameed. 2016. Antibacterial effect of ginger (zingiber officinale) roscoe and bioactive chemical analysis using gas chromatography mass spectrum. *Orient. J. Chem.*, 32(2): 20-40.

Shoge, M. and T. Amusan. 2020. Phytochemical, antidiarrhoeal activity, isolation and characterisation of 11-octadecenoic acid, methyl ester isolated from the seeds of *Acacia nilotica* Linn. *J .Biotechnol. Immun.*, 2: 1-12.

Soliman, M.I., M.S. Zaghloul and Y.M. Heikal. 2014. Genetic variation within and among three egyptian mesembryanthemum species using different genetic markers. *Egypt. J. Basic Appl. Sci.*, 1(3-4): 127-135.

Sosa, A.A., S.H. Bagi and I.H. Hameed. 2016. Analysis of bioactive chemical compounds of euphorbia lathyrus using gas chromatography-mass spectrometry and fourier-transform infrared spectroscopy. *J. Pharmacog. Phytother.*, 8(5): 109-126.

Sun, H., J. Ding, M. Piednoël and K. Schneeberger. 2017. Findgse: Estimating genome size variation within human and arabidopsis using k-mer frequencies. *Bioinformatics*, 34(4): 550-557.

Sun, Y., M.E. Netzel, D. Sivakumar and Y. Sultanbawa. 2025. Climate-smart Halophyte: The role of Atriplex in future food security. *TIFS*, 156: 104869.

Sundarraj, S., R. Thangam, V. Sreevani, K. Kaveri, P. Gunasekaran, S. Achiraman and S. Kannan. 2012. γ-sitosterol from *Acacia nilotica* L. Induces g2/m cell cycle arrest and apoptosis through c-myc suppression in mcf-7 and a549 cells. *J. Ethnopharmacol*., 141(3): 803-809.

Sunday, U.E., M.I. Stephanie, F. Otuonye, D. Oluwadamilola and A.A. Lazarus. 2025. Computational investigation of stigmasterol as a potential therapeutic agent for cervical cancer: Insights from density functional theory (dft) and molecular docking studies. *In Silico Pharmacol.,* 13(2): 77.

Suresh, A., R. Praveenkumar, R. Thangaraj, F.L. Oscar, E. Baldev, D. Dhanasekaran and N. Thajuddin. 2014. Microalgal fatty acid methyl ester a new source of bioactive compounds with antimicrobial activity. *Asian Pac. J. Trop. Dis.,* 4: S979-S984.

Tripathi, N., S. Kumar, R. Singh, C. Singh, P. Singh and V. Varshney. 2013. Isolation and identification of γ-sitosterol by GC-MS from the leaves of *Girardinia heterophylla* (decne). *Open Bioact. Compd. J.*, 4: 25-27.

Vijayan, K. 2005. Inter simple sequence repeat (ISSR) polymorphism and its application in mulberry genome analysis. *Int. J. Indus. Entomol.,* 10(2): 79-86.

Wade, A.G., G.M. Crawford, D. Young, S. Corson and C. Brown. 2019. Comparison of diclofenac gel, ibuprofen gel, and ibuprofen gel with levomenthol for the topical treatment of pain associated with musculoskeletal injuries. *J. Int. Med. Res.*, 47(9): 4454-4468.

Wang, K., P. Jin, S. Cao, H. Shang, Z. Yang and Y. Zheng. 2009. Methyl jasmonate reduces decay and enhances antioxidant capacity in chinese bayberries. *J. Agric.Food Chem.,* 57(13): 5809-5815.

Wang, X., J.A. Morton, J. Pellicer, I.J. Leitch and A.R. Leitch. 2021. Genome downsizing after polyploidy: Mechanisms, rates and selection pressures. *Plant J.*, 107(4): 1003-1015.

Wyson, J.W., M. Deventhiran, P. Saravanan, D. Anand and S. Rajarajan. 2016. Phytochemical analysis of leaf extract of *Eclipta prostrata* (L.) by gc-ms method. *Int. J. Pharm. Sci. Res.,* 7(1): 272.

Yang, C., R. Halitschke and S.E. O'Connor. 2024. Oxidosqualene cyclase 1 and 2 influence triterpene biosynthesis and defense in *Nicotiana attenuata*. *Plant Physiol.*, 194(4): 2580-2599.

Yıldırım, E., M. Türkkan, S. Derviş, N. Dalbastı, G. Özer and İ. Erper. 2024. In vitro evaluation of salt-based antifungal compounds for sustainable control of neoscytalidium dimidiatum. *Akademik Ziraat Dergisi*, 13(2): 298-309.

Youssef, A.M.M., D.A.M. Maaty and Y.M. Al-Saraireh. 2023. Phytochemical analysis and profiling of antitumor compounds of leaves and stems of *Calystegia silvatica* (kit.) griseb. *Molecules*, 28(2): 630.

Zamani, Z., R. Tamartash, Q. Heydari and Z.J. Jelodar. 2025. Impact of soil factors and climate on phytochemical characteristics of *Stachys lavandulifolia* Vahl. *Chem. Biodiv.*, 22(5): e202402352.

Zietkiewicz, E., A. Rafalski and D. Labuda. 1994. Genome fingerprinting by simple sequence repeat (SSR)-anchored polymerase chain reaction amplification. *Genomics,* 20(2): 176-183.